Analysing $gg \to h \to Z\gamma$ decay at the LHC using SMEFT

Njokweni Mbuyiswa[1,2], Kutlwano Makgetha[1,2], Srimoy Bhattacharya[1], Abdualazem Fadol[1,3], Katlego Machete[1,2], Mukesh Kumar[1], and Bruce Mellado[1,2]

[1] School of Physics and Institute for Collider Particle Physics, University of the Witwatersrand, Johannesburg, Wits 2050, South Africa.
[2] iThemba LABS, National Research Foundation, PO Box 722, Somerset West 7129, South Africa.
[3]Institute of High Energy Physics, Chinese Academy of Sciences, 19B Yuquan Road, Shijingshan District, Beijing, China

E-mail: 2314612@students.wits.ac.za

Abstract. The ATLAS and CMS collaborative effort resulted in the first evidence of the Higgs boson (h) decay into a Z-boson and a photon, with a statistical significance of 3.4σ. The measured signal rate relative to the SM prediction was found to be 2.2 ± 0.7 times the leading order Standard Model (SM) prediction. Recent study shows that even with next-to-leading order QCD corrections and the signal-background interference, this excess in $h \to Z\gamma$ cannot be explained within the SM. With this motivation we perform our analysis of the above-mentioned process through gluon-fusion and constraint the corresponding six-dimension Wilson coefficients in SMEFT through the cross section measurement and different sensitive kinematic observables. For this study we consider $Z \to \ell^+\ell^-$ ($\ell^\pm = e^\pm, \mu^\pm$).

1 Introduction

The initial indication of the decay of the Higgs boson into a photon and a Z boson is unveiled, with a statistical significance of 3.4σ [1]. This finding stems from a joint examination of the exploration efforts carried out in collaborations of CMS and ATLAS using proton-proton collision datasets amassed at the Large Hadron Collider (LHC) at CERN. The datasets represent a centre-of-mass energy of 13 TeV with an accumulated luminosity of approximately 140 fb $^{-1}$ for both experiments. The observed signal count amounts to 2.2 ± 0.7 times the prediction of the Standard Model (SM) [1]. In the SM it is expected to possess a relatively minor branching fraction of approximately $\sim (1.5 \pm 0.1) \times 10^{-3}$ for when the Higgs boson mass is close to 125 GeV ($m_h \approx 125$ GeV) [2, 3]. Since the $h \to Z\gamma$ decay transpires through loop diagrams, as depicted in Figure 1 it is susceptible to alterations in numerous Beyond the Standard Model (BSM) implications, potentially leading to a relatively greater branching fraction when it is being compared to the prediction in the SM. The framework with the most potential to explain these deviations to date is the Standard Model Effective Field Theory (SMEFT). This is a framework that expands upon the Standard Model by incorporating higher-dimensional operators that are repressed by a new physics scale Λ [4]. These operators are constructed using the SM fields and adhere to the SM gauge symmetries. The SMEFT Lagrangian is given by:

$$\mathcal{L}_{\text{SMEFT}} = \mathcal{L}_{\text{SM}} + \sum_{d>4} \sum_{i} \frac{C_i(d)}{\Lambda^{d-4}} \mathcal{O}_i(d), \tag{1}$$

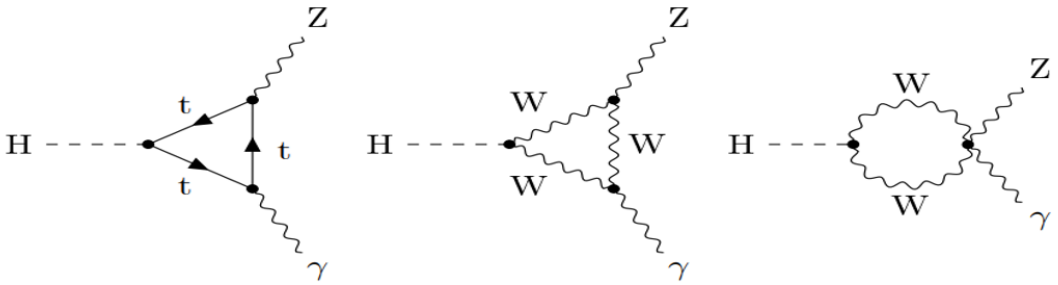

Figure 1: The first diagram (a) include contributions from a top quark loop shows the vertex for this decay. The diagrams (b) and (c) represent loop contributions involving W bosons.

where $\mathcal{L}_{\text{SM}}$ is the SM Lagrangian, d is the mass dimension of the operators, $C_i(d)$ are the Wilson coefficients, and $\mathcal{O}_i(d)$ are the higher-dimensional operators. The relevant operators and their Wilson coefficients, determined for this analysis that contribute the $h \to Z\gamma$ decay vertex, are:

$$\texttt{cpBB}(C_B) \to O_{\varphi B} = (\varphi^+\varphi - \frac{v^2}{2})B^{\mu\nu}B_{\mu\nu}, \tag{2}$$

$$\texttt{cpWB}(C_{WB}) \to O_{\varphi WB} = (\varphi^+\tau_I\varphi)B^{\mu\nu}W^I_{\mu\nu}, \tag{3}$$

$$\texttt{cpW}(C_W) \to O_{\varphi W} = (\varphi^+\varphi - \frac{v^2}{2})W^{\mu\nu}_I W^I_{\mu\nu}, \tag{4}$$

The SMEFT framework provides a powerful tool for studying the effects of new physics beyond the SM in a model-independent manner. By systematically including higher-dimensional operators up to a certain mass dimension, one can explore the implications of new physics at different energy scales. For the preliminary results, we consider the case where the relevant operators are all set to 1.

2 Monte Carlo Event Generation

Simulated proton-proton collision events were generated with MADGRAPH5 [5] for both signal and major background processes. Parton showering, hadronization, and underlying event modeling were handled using PYTHIA8 [6], ensuring the final state particles resulting from the hard scattering processes were realistically simulated. These events were processed through the DELPHES3.4.2 [7] to model detector responses and effects accurately. Jets were clustered using FASTJET [8] with the anti-k_T algorithm [9], employing a distance parameter of $R = 0.4$. The factorization and normalization scales were dynamically set for both signal and background processes. The focus of this analysis is on the decay of the Higgs boson into a Z boson and a photon, $h \to Z\gamma$. The first step involves identifying the higher-dimensional operators contributing to this decay channel within the framework of the SMEFT [10]. The relevant operators were derived following the formulation outlined in [11], where one-loop electroweak corrections to this decay process are calculated. The Wilson coefficients for these operators were obtained using the `SMEFT@NLO` package [12], which leverages models developed in `FeynRules` [13]. MC event generation was performed for both signal and background processes using a combination of tools. The signal process $gg \to h \to Z\gamma$ was generated and interfaced with the `SMEFT@NLO` model. This process corresponds to the decay of the Higgs boson into a photon (γ) and a Z boson, as predicted by the SMEFT framework. The background processes considered in the analysis include several SM interactions that could mimic the signal. These background processes considered are $pp \to \ell^+\ell^-\gamma$, representing the background from dilepton pair production accompanied by a photon for the dilepton final state of the signal; $pp \to jj\gamma$, representing the background from the production of two light-flavor jets with a photon for the dijet final state of the signal; $pp \to b\bar{b}\gamma$, representing the background from the production of two b-tagged jets with a photon for di$b$-jet final state of the signal; and $pp \to$ MET $+ \gamma$, representing the background from the production of missing transverse energy (MET) due to neutrinos, also accompanied by a photon for the di-neutrino final state for the signal. Jets within $\Delta R = 0.2$ of leptons or photons were excluded. Electrons were also removed if they were within $\Delta R = 0.02$ of muons or other electrons. These object definitions defined in Table 1 were essential for ensuring accurate and efficient simulation of the signal and background processes, serving as a foundation for the analysis of the $h \to Z\gamma$ decay within the SMEFT framework. The selection criteria for the case whereby the Z decays into two oppositely charged leptons of the same flavour are described in Table 2.

Object	Pseudorapidity ($\lvert\eta\rvert$)	Transverse Momentum (p_T)
Muons	$\lvert\eta_\mu\rvert < 2.7$	$p_{\mathrm{T}}^{\mu} > 10$ GeV
Electrons	$\lvert\eta_e\rvert < 2.47$ (excluding $1.37 < \lvert\eta_e\rvert < 1.52$)	$p_{\mathrm{T}}^{e} > 10$ GeV
Photons	$\lvert\eta_\gamma\rvert < 2.47$ (excluding $1.37 < \lvert\eta_\gamma\rvert < 1.52$)	$p_{\mathrm{T}}^{\gamma} > 10$ GeV
Jets	Anti-k_t with $\Delta R = 0.4$, $\lvert\eta_j\rvert < 4.4$	$p_{\mathrm{T}}^{j} > 25$ GeV

Table 1: Object definitions at the generator level.

Selection Category	Criteria
Photon Selection	At least one photon must satisfy the object definition criteria.
Lepton Selection	Two same-flavor, opposite-sign leptons (electrons or muons) must satisfy the object definition criteria.
Z Boson Reconstruction	Invariant mass of the lepton pair within 81 GeV $< m_{\ell\ell} <$ 101 GeV.
Transverse Momentum of $Z\gamma$ System	p_{T} of the $Z\gamma$ system > 50 GeV to reduce background.
ΔR Cuts	Angular separation cuts such as $\Delta R(\gamma, \ell) > 0.4$ to ensure well-separated objects.
Missing Transverse Energy	If applicable, require MET < 40 GeV to reduce background from processes involving neutrinos.

Table 2: Selection Criteria for $Z\gamma$ analysis whereby the Z decays into two oppositely charged leptons of the same flavour

3 Preliminary results

As described in the object definitions and selection criteria, we select events with exactly two leptons and one photon. The distributions in Figure 2 show that a bulk of our generated samples for both the background and signal fit that criteria. In putting the events through the other cuts we plot the distributions scaled to unity in order to make a distinction in where the signal and background peaks. For the distributions of the $m_{\ell\ell}$ and $m_{Z\gamma}$ in Figure 3, we plan to perform a Gaussian fit at least two standard deviation from their peak in order to find their resolution.

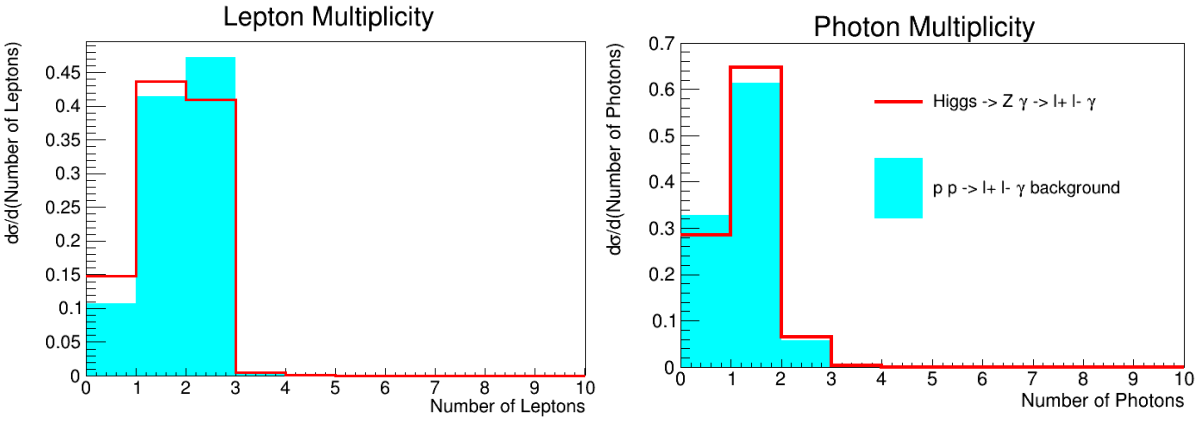

Figure 2: These are the distributions of the photon and lepton multiplicity after the object definition criteria. As expected from the MC generated samples, there are more events that have two leptons and one photon.

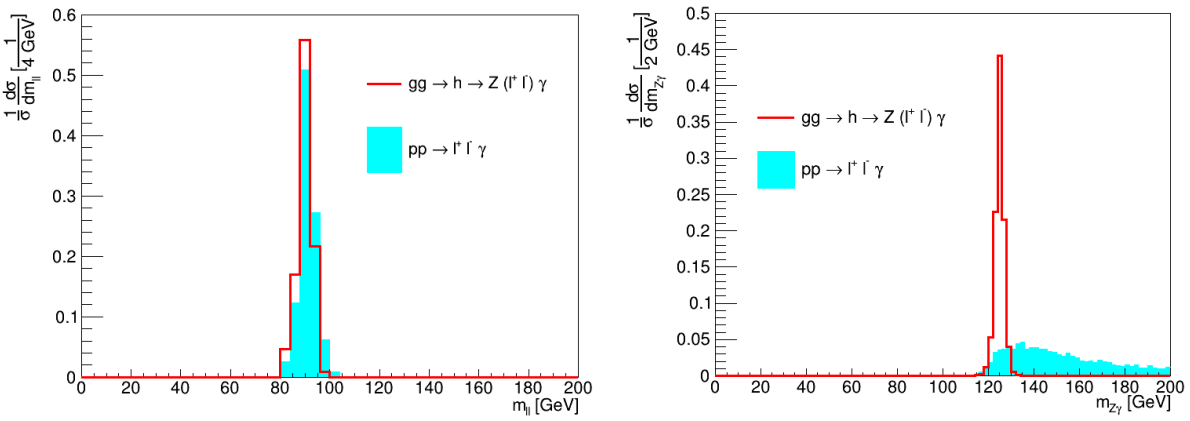

Figure 3: The distribution of $m_{\ell\ell}$ system (*left*) peaks around the Z mass of 90 GeV after the minimal selection criteria as expected. The distribution of the $m_{Z\gamma}$ system (*right*) after the selection criteria peaks at about the higgs boson mass as expected.

4 Conclusion and Future Plans

This work represents an ongoing effort to extract meaningful constraints on dimension-six operators in the SMEFT through the study of the rare decay process $h \to Z\gamma$. Based on the preliminary results shown in Figure 3, our aim is to refine the resolution of the differential distributions by optimizing the invariant mass window, thus improving the signal-to-background ratio. Our future analysis will employ both inclusive and bin-by-bin differential approaches to constrain the SMEFT Wilson coefficients. In the inclusive method, we will integrate over all kinematic regions of interest, whereas in the bin-by-bin method, we will analyze individual bins of the differential distribution, allowing for improved sensitivity to deviations from SM predictions in specific kinematic regions. Subsequent steps involve reweighting the differential distributions using corrected cross sections derived from constrained values of the SMEFT Wilson coefficients. These constraints will be determined by computing the decay amplitude for the $h \to Z\gamma$ process within the SMEFT framework, incorporating contributions from relevant Feynman diagrams. Comparison with experimental measurements will allow us to fit the Wilson coefficients using a χ^2 minimization procedure, defined as:

$$\chi^2 = \sum_{k=1}^{n} \left(\frac{\sigma_k^{\text{BSM}} - \sigma_k^{\text{SM}}}{\Delta\sigma_k} \right)^2 \text{with} \Delta\sigma_k = \sqrt{\frac{\sigma_k^{\text{SM}}}{\mathcal{L}} + \left(\delta_s\, \sigma_k^{\text{SM}}\right)^2}, \tag{5}$$

where $\mathcal{L}$ is the integrated luminosity, σ_k is the cross section in the kth bin of a distribution of n-bins and δ_s is the systematic uncertainty. The cross section in the presence of new physics contributions can be expressed in quadratic form as [14, 15, 16, 17]:

$$\sigma^{\text{BSM}} = \sigma^{\text{SM}} + \sum_i C_i A_i + \sum_{i,j} C_i C_j B_{ij},$$

where C_i are the Wilson coefficients, and the parameters A_i, B_{ij} capture the interference and pure BSM contributions respectively. To obtain robust and realistic constraints on the BSM couplings, we plan to perform a multi-parameter analysis by simultaneously varying all relevant SMEFT Wilson coefficients within a benchmark range of $[-1, 1]$, extracting the posterior distributions after marginalization using a Markov Chain Monte Carlo (MCMC) technique. The analysis will utilize a binned sensitive distribution which we will find determine using Random Forest classification [18] algorithm. We will be applying the `GetDist` package [19] to extract credible intervals and plot posterior projection while accounting for any correlations and degeneracies found among the parameters in the multidimensional space. We will also set exclusion limits at the 95 percent confidence level on the Wilson coefficients. In parallel, we plan to extend this analysis to other final states where the Z boson decays into hadronic jets ($Z \to jj$), b-tagged jets ($Z \to b\bar{b}$), and neutrinos ($Z \to \nu\bar{\nu}$), each with their own dominant background processes and associated systematics. These additional channels are expected to increase overall sensitivity to SMEFT effects. We will also investigate other Higgs production modes beyond gluon fusion, including Vector Boson Fusion (VBF), associated production with a vector boson (VH), and associated production with top quarks ($t\bar{t}H$), to explore operator structures not fully accessible in a single production mechanism. These steps will collectively provide a more comprehensive probe of electroweak interactions and possible new physics effects within the SMEFT framework using the rare $h \to Z\gamma$ decay channel.

References

[1] G. Aad *et al.*, "Evidence for the Higgs Boson Decay to a Z Boson and a Photon at the LHC," *Phys. Rev. Lett.*, vol. 132, no. 2, p. 021803, 2024.

[2] A. Djouadi, J. Kalinowski, and M. Spira, "Hdecay: A program for higgs boson decays in the standard model and its supersymmetric extension," *Computer Physics Communications*, vol. 108, no. 1, pp. 56–74, 1998.

[3] D. de Florian, D. Fontes, J. Quevillon, M. Schumacher, F. Llanes-Estrada, A. Gritsan, E. Vryonidou, A. Signer, P. de Castro Manzano, D. Pagani *et al.*, *arXiv: Handbook of LHC Higgs Cross Sections: 4. Deciphering the Nature of the Higgs Sector*. Cern, 2016, no. arXiv: 1610.07922.

[4] G. Passarino and M. Trott, "The standard model effective field theory and next to leading order," *arXiv preprint arXiv:1610.08356*, 2016.

[5] J. Alwall, R. Frederix, S. Frixione, V. Hirschi, F. Maltoni, O. Mattelaer, H.-S. Shao, T. Stelzer, P. Torrielli, and M. Zaro, "The automated computation of tree-level and next-to-leading order differential cross sections, and their matching to parton shower simulations," *Journal of High Energy Physics*, vol. 2014, no. 7, pp. 1–157, 2014.

[6] T. Sjöstrand, S. Ask, J. R. Christiansen, R. Corke, N. Desai, P. Ilten, S. Mrenna, S. Prestel, C. O. Rasmussen, and P. Z. Skands, "An introduction to pythia 8.2," *Computer physics communications*, vol. 191, pp. 159–177, 2015.

[7] J. De Favereau, C. Delaere, P. Demin, A. Giammanco, V. Lemaitre, A. Mertens, and M. Selvaggi, "Delphes 3: a modular framework for fast simulation of a generic collider experiment," *Journal of High Energy Physics*, vol. 2014, no. 2, pp. 1–26, 2014.

[8] M. Cacciari, G. P. Salam, and G. Soyez, "FastJet User Manual," *Eur. Phys. J. C*, vol. 72, p. 1896, 2012.

[9] M. Cacciari, G. P. Salam, and Soyez, "The anti-k_t jet clustering algorithm," *JHEP*, vol. 04, p. 063, 2008.

[10] Z.-Q. Chen, L.-B. Chen, C.-F. Qiao, and R. Zhu, "Two-loop electroweak corrections to the higgs boson rare decay process $h \to z\gamma$," 2024.

[11] S. Dawson and P. P. Giardino, "Higgs decays to z z and z γ in the standard model effective field theory: An nlo analysis," *Physical Review D*, vol. 97, no. 9, p. 093003, 2018.

[12] C. Degrande, G. Durieux, F. Maltoni, K. Mimasu, E. Vryonidou, and C. Zhang, "Automated one-loop computations in the standard model effective field theory," *Physical Review D*, vol. 103, no. 9, p. 096024, 2021.

[13] A. Alloul, N. D. Christensen, C. Degrande, C. Duhr, and B. Fuks, "Feynrules 2.0—a complete toolbox for tree-level phenomenology," *Computer Physics Communications*, vol. 185, no. 8, pp. 2250–2300, 2014.

[14] R. Rahaman, "On two-body and three-body spin correlations in leptonic $t\bar{t}Z$ production and anomalous couplings at the LHC," *JHEP*, vol. 02, p. 077, 2023.

[15] K. Mosala, P. Sharma, M. Kumar, and A. Goyal, "Axion-like particles at future $e^{-}p$ collider," *Eur. Phys. J. C*, vol. 84, no. 1, p. 44, 2024.

[16] R. Rahaman and R. K. Singh, "Unravelling the anomalous gauge boson couplings in $ZW^{\pm}$ production at the LHC and the role of spin-1 polarizations," *JHEP*, vol. 04, p. 075, 2020.

[17] B. Ravina, E. Simpson, and J. Howarth, "Observing $t\bar{t}Z$ spin correlations at the LHC," *Eur. Phys. J. C*, vol. 81, no. 9, p. 809, 2021.

[18] A. Iqbal, J. Verboncoeur, and P. Zhang, "A Supervised Machine Learning Framework for Multipactor Breakdown Prediction in High-Power Radio Frequency Devices and Accelerator Components: A Case Study in Planar Geometry," 7 2025.

[19] A. Lewis, "GetDist: a Python package for analysing Monte Carlo samples," 10 2019.